ISSN 0081-5438, Proceedings of the Steklov Institute of Mathematics, 2016, Vol. 295, pp. 158–167. © Pleiades Publishing, Ltd., 2016.
Original Russian Text © Yu.L. Karavaev, A.A. Kilin, 2016, published in Trudy Matematicheskogo Instituta imeni V.A. Steklova, 2016, Vol. 295, pp. 174–183.

Nonholonomic Dynamics and Control of a Spherical Robot with an Internal Omniwheel Platform: Theory and Experiments

Yu. L. Karavaev [a,b] **and A. A. Kilin** [b]

Received June 29, 2016

Abstract—We present the results of theoretical and experimental investigations of the motion of a spherical robot on a plane. The motion is actuated by a platform with omniwheels placed inside the robot. The control of the spherical robot is based on a dynamic model in the nonholonomic statement expressed as equations of motion in quasivelocities with indeterminate coefficients. A number of experiments have been carried out that confirm the adequacy of the dynamic model proposed.

DOI: 10.1134/S0081543816080095

1. INTRODUCTION

The study of the motion of spherical robots has recently become a popular trend, which is confirmed by a large number of publications. There are several tens of various designs, which are classified and described in [1, 2, 9–12, 14–19] and other papers. The control of such systems is a complicated and interesting problem in the field of dynamics of many-body systems. Note that the interaction between the components of a spherical robot can be described by both holonomic (in case of an internal pendulum) and nonholonomic (internal wheel platforms) constraints. This fact distinguishes such systems from other systems, for example, trailers, where only the constraints corresponding to the interaction of the body with the underlying surface are nonholonomic. For the recent studies on the motion of spherical robots that use the basic nonholonomic model, see [4, 13, 14, 20, 21]. In these studies, one can find comprehensive literature on spherical robots and related problems. Although a nonholonomic model often leads to errors in the description of the motion of mechanical systems, it nevertheless allows one to construct adequate control laws. An important problem here is to determine conditions under which the application of a nonholonomic model in experimental investigations is justified. This issue is discussed in detail in [3, 6–8].

The results of experimental and theoretical investigations of a spherical robot with an internal omniwheel platform presented in this paper are the logical conclusion of the authors' study [14], where the derivation of equations of motion was thoroughly described and their analysis was carried out. In [14], a numerical simulation was also performed and trajectories of a spherical robot with an internal omniwheel platform were constructed. In Sections 2 and 3, we give a brief account of the kinematic and dynamic models of the system on the basis of nonholonomic equations of motion with the use of quasicoordinates. In Section 4, we describe an algorithm for constructing a control that guarantees a steady motion of a spherical robot before and after executing a manoeuvre corresponding to this control. In Section 5, we present the results of comparison of

[a] Kalashnikov Izhevsk State Technical University, ul. Studencheskaya 7, Izhevsk, 426069 Russia.

[b] Udmurt State University, ul. Universitetskaya 1, Izhevsk, 426034 Russia.

E-mail addresses: karavaev_yury@istu.ru (Yu.L. Karavaev), aka@rcd.ru (A.A. Kilin).

experimental trajectories of the controlled motion of a spherical robot within the kinematic and dynamic models. We also analyze the experimental trajectories and compare them with the results of simulation.

2. KINEMATICS OF A SPHERICAL ROBOT WITH AN INTERNAL OMNIWHEEL PLATFORM

We model a spherical robot that moves on the horizontal plane as a system of bodies consisting of a spherical shell of radius R_0 and a platform inside it with three identical omniwheels of radius R_{w} (Fig. 1). In this paper, by omniwheels we mean the Mechanum wheels, whose design and nonholonomic model are described in [5]. Namely, an omniwheel is modeled by a plane disk for which the velocity of the contact point with the underlying surface is directed along a straight line making a constant angle with the plane of the wheel.

To describe the motion of the spherical robot, consider three systems of coordinates. The first $OXYZ$ is fixed and has unit vectors $\boldsymbol{\alpha}$, $\boldsymbol{\beta}$, and $\boldsymbol{\gamma}$; the second $Cx'y'z'$ is movable, rigidly bound to the spherical shell, and has unit vectors $\boldsymbol{\xi}$, $\boldsymbol{\eta}$, and $\boldsymbol{\zeta}$; and the third $Cxyz$ is movable, rigidly bound to the omniwheel platform, and has unit vectors $\mathbf{e}_1$, $\mathbf{e}_2$, and $\mathbf{e}_3$ (see Fig. 1b). The design of the moving platform is described by the following constant (in the coordinate system $Cxyz$) vectors: $\mathbf{r}_i$, the radius vectors of the centers of omniwheels; $\mathbf{n}_i$, the unit vectors directed along the rotation axes of omniwheels; $\boldsymbol{\alpha}_i$, the unit vectors that define the directions of the rotation axes of the rollers of each wheel at the contact points with the shell; and $\mathbf{r}_{\mathrm{m}}$, the vector defining the position of the center of mass of the moving platform with omniwheels.

We will define the position of the system by the coordinates of the center of the spherical shell in the fixed system of coordinates $\mathbf{r} = (x, y, 0)$, by the angles of rotation of the wheels $\boldsymbol{\chi} = (\chi_1, \chi_2, \chi_3)$, and by two matrices that define the spatial orientation of the platform and the spherical shell:

$$\mathbf{Q} = (\boldsymbol{\alpha}, \boldsymbol{\beta}, \boldsymbol{\gamma}), \qquad \mathbf{S} = (\boldsymbol{\xi}, \boldsymbol{\eta}, \boldsymbol{\zeta}). \tag{2.1}$$

Henceforth (unless otherwise stated), all vectors are expressed in terms of the projections to the axes of the coordinate system $Cxyz$, which is rigidly bound to the platform.

In these coordinates, the motion of the spherical shell and the platform is described by the following kinematic relations:

$$\dot{\mathbf{r}} = \mathbf{Q}^{\mathrm{T}}\mathbf{v}, \qquad \dot{\mathbf{Q}} = \widetilde{\boldsymbol{\omega}}\mathbf{Q}, \qquad \dot{\mathbf{S}} = (\widetilde{\boldsymbol{\omega}} - \widetilde{\boldsymbol{\Omega}})\mathbf{S}, \tag{2.2}$$

where $\mathbf{v}$ is the velocity of the center of the sphere (in the projections onto the axes of the system $Cxyz$) and matrices $\widetilde{\boldsymbol{\omega}}$ and $\widetilde{\boldsymbol{\Omega}}$ are expressed in terms of the components of the absolute angular velocities of the moving platform $\boldsymbol{\omega}$ and the spherical shell $\boldsymbol{\Omega}$ as follows:

$$\widetilde{\boldsymbol{\omega}} = \begin{pmatrix} 0 & \omega_3 & -\omega_2 \\ -\omega_3 & 0 & \omega_1 \\ \omega_2 & -\omega_1 & 0 \end{pmatrix}, \qquad \widetilde{\boldsymbol{\Omega}} = \begin{pmatrix} 0 & \Omega_3 & -\Omega_2 \\ -\Omega_3 & 0 & \Omega_1 \\ \Omega_2 & -\Omega_1 & 0 \end{pmatrix}.$$

Here, $\boldsymbol{\omega}$, $\boldsymbol{\Omega}$, and $\mathbf{v}$ are quasivelocities, and their relation to generalized velocities is given by formulas (2.2).

We will assume that the system moves without slipping at the points of contact of the spherical shell with the plane and the omniwheels. This imposes nonholonomic constraints on the system. The nonslipping of the spherical shell on the plane yields the constraint

$$\mathbf{F} = \mathbf{v} - R_0\boldsymbol{\Omega} \times \boldsymbol{\gamma} = 0, \tag{2.3}$$

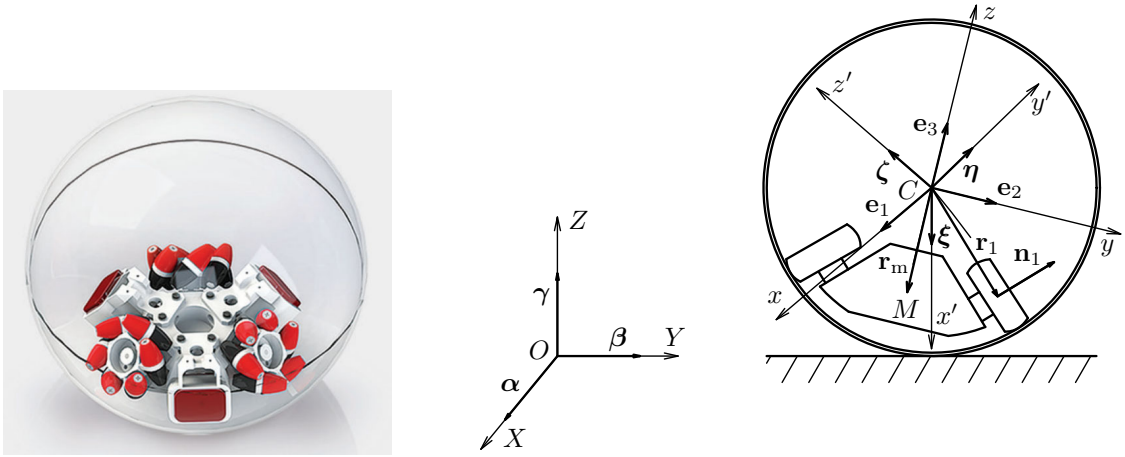

(a) (b)

Fig. 1. (a) A three-dimensional model of a spherical robot with an internal omniwheel platform and (b) a scheme of the spherical robot.

and the nonslipping of the wheels on the spherical shell yields [5] the constraint

$$G_i = \dot{\chi}_i + \frac{R_0}{(\mathbf{s}_i, \mathbf{n}_i)R_{\mathrm{w}}}(\boldsymbol{\omega} - \boldsymbol{\Omega}, \mathbf{s}_i) = 0, \tag{2.4}$$

where $\mathbf{s}_i = \mathbf{r}_i \times \boldsymbol{\alpha}_i$.

Within the kinematic model, the following assumptions are made in [14].

1. During the motion of the spherical robot, the center of mass of the platform always occupies the lowest possible position. Then the radius vector of the center of mass can be represented as

$$\mathbf{r}_{\mathrm{m}} = -R_{\mathrm{m}}\boldsymbol{\gamma}, \tag{2.5}$$

where R_{m} is the distance from the origin of the moving system of coordinates to the center of mass of the moving platform.

2. Under the first assumption, the constant nutation angles $\theta = \theta_{\mathrm{m}}$ and proper rotation angles $\varphi = \varphi_{\mathrm{m}}$ define, up to sign, the spherical coordinates of the center of mass of the platform with omniwheels in the moving system of coordinates. Singling out the corresponding constant factor in the matrix $\mathbf{Q}$, we obtain

$$\mathbf{Q} = \mathbf{Q}_{\mathrm{m}}\mathbf{Q}_{\psi}, \tag{2.6}$$

where the matrix $\mathbf{Q}_{\mathrm{m}}$ has the form

$$\mathbf{Q}_{\mathrm{m}} = \begin{pmatrix} \cos\varphi_{\mathrm{m}} & \cos\theta_{\mathrm{m}}\sin\varphi_{\mathrm{m}} & \sin\theta_{\mathrm{m}}\sin\varphi_{\mathrm{m}} \\ -\sin\varphi_{\mathrm{m}} & \cos\theta_{\mathrm{m}}\cos\varphi_{\mathrm{m}} & \sin\theta_{\mathrm{m}}\cos\varphi_{\mathrm{m}} \\ 0 & -\sin\theta_{\mathrm{m}} & \cos\theta_{\mathrm{m}} \end{pmatrix} \tag{2.7}$$

and the matrix

$$\mathbf{Q}_{\psi} = \begin{pmatrix} \cos\psi & \sin\psi & 0 \\ -\sin\psi & \cos\psi & 0 \\ 0 & 0 & 1 \end{pmatrix} \tag{2.8}$$

corresponds to the rotation of the moving platform about the vertical axis with a precession angle ψ.

Within the kinematic model, the role of controls is played by the angular velocities $\dot\chi_i$ of the omniwheels. Expressing $\boldsymbol\Omega$ from the constraint equation (2.3) and taking into account the assumptions made, we obtain a formula for the angular velocities of the wheels that realize a motion along the trajectory $\mathbf{r}_{\mathrm{c}}(t)$ with a given function $\Omega_\gamma(t)$:

$$\dot\chi_i = \frac{1}{R_{\mathrm{w}}}\frac{(\mathbf{Q}_{\mathrm{m}}^{\mathrm{T}}\mathbf{s}_i, \mathbf{e}_3\times\mathbf{Q}_\psi^{\mathrm{T}}\dot{\mathbf{r}}_{\mathrm{c}} + R_0(\Omega_\gamma-\omega_\gamma)\mathbf{e}_3)}{(\mathbf{s}_i,\mathbf{n}_i)}. \tag{2.9}$$

Here the angular velocity ω_γ is a free parameter; i.e., within the kinematic model, one can realize the motion along a given trajectory up to an arbitrary rotation $\omega_\gamma(t)$ of the platform about the vertical axis.

When carrying out experiments, just as in [14], we consider the motion of the spherical shell within the "rubber" rolling model; i.e., we assume that $\Omega_\gamma\equiv 0$.

3. DYNAMICS OF A SPHERICAL ROBOT WITH AN INTERNAL OMNIWHEEL PLATFORM

Now, consider the solution of the problem of controlling a spherical robot within the dynamic model. For the above-described model of a spherical robot, we write equations of motion in quasivelocities $(\boldsymbol\omega,\boldsymbol\Omega,\mathbf{v},\dot{\boldsymbol\chi})$ while taking account of nonholonomic constraints and control:

$$\begin{aligned}
\frac{d}{dt}\left(\frac{\partial L}{\partial\boldsymbol\omega}\right) &= \frac{\partial L}{\partial\boldsymbol\omega}\times\boldsymbol\omega + \frac{\partial L}{\partial\mathbf{v}}\times\mathbf{v} + \frac{\partial L}{\partial\boldsymbol\gamma}\times\boldsymbol\gamma + \left(\frac{\partial\mathbf{G}}{\partial\boldsymbol\omega}\right)^{\mathrm{T}}\widetilde{\boldsymbol\lambda},\\
\frac{d}{dt}\left(\frac{\partial L}{\partial\boldsymbol\Omega}\right) &= \frac{\partial L}{\partial\boldsymbol\Omega}\times\boldsymbol\omega + \left(\frac{\partial\mathbf{G}}{\partial\boldsymbol\Omega}\right)^{\mathrm{T}}\widetilde{\boldsymbol\lambda} + \left(\frac{\partial\mathbf{F}}{\partial\boldsymbol\Omega}\right)^{\mathrm{T}}\boldsymbol\lambda,\\
\frac{d}{dt}\left(\frac{\partial L}{\partial\mathbf{v}}\right) &= \frac{\partial L}{\partial\mathbf{v}}\times\boldsymbol\omega + \left(\frac{\partial\mathbf{F}}{\partial\mathbf{v}}\right)^{\mathrm{T}}\boldsymbol\lambda,\\
\frac{d}{dt}\left(\frac{\partial L}{\partial\dot\chi}\right) &= \frac{\partial L}{\partial\chi} + \left(\frac{\partial\mathbf{G}}{\partial\dot\chi}\right)^{\mathrm{T}}\widetilde{\boldsymbol\lambda} + \mathbf{K}.
\end{aligned} \tag{3.1}$$

Here L is the Lagrange function, $\boldsymbol\lambda=(\lambda_1,\lambda_2,\lambda_3)$ and $\widetilde{\boldsymbol\lambda}=(\widetilde\lambda_1,\widetilde\lambda_2,\widetilde\lambda_3)$ are indeterminate Lagrange multipliers, $\mathbf{K}=(K_1,K_2,K_3)$ is the vector of control moments, where K_i is the moment of forces applied to the axis of the ith wheel, and $\mathbf{F}$ and $\mathbf{G}$ are the nonholonomic constraints (2.3) and (2.4).

The kinetic energy of the system can be represented as a sum of three terms: the kinetic energy of the spherical shell T_0, the kinetic energy of the platform T_{p}, and the kinetic energy of the wheels T_i:

$$\begin{aligned}
T &= T_0 + T_{\mathrm{p}} + \sum_{i=1}^{3} T_i\\
&= \frac{1}{2}(m+m_0)\mathbf{v}^2 + \frac{1}{2}I_0\boldsymbol\Omega^2 + \frac{1}{2}(\boldsymbol\omega,\mathbf{I}\boldsymbol\omega) + m(\mathbf{v},\boldsymbol\omega\times\mathbf{r}_{\mathrm{m}}) + \sum_{i=1}^{3} j\dot\chi_i(\boldsymbol\omega,\mathbf{n}_i) + \frac{1}{2}\sum_{i=1}^{3} j\dot\chi_i^2,
\end{aligned} \tag{3.2}$$

where $m=m_{\mathrm{p}}+\sum_{i=1}^3 m_i$ is the mass of the moving platform with omniwheels, m_0 and I_0 are the mass and the central inertia tensor of the spherical shell, m_{p} and $\mathbf{I}_{\mathrm{p}}$ are the mass of the moving platform and its tensor of inertia with respect to the center of the sphere, $\mathbf{r}_{\mathrm{p}}$ is the radius vector from the center of the sphere to the center of mass of the platform (without omniwheels), $\mathbf{r}_{\mathrm{m}}=\bigl(m_{\mathrm{p}}\mathbf{r}_{\mathrm{p}}+\sum_{i=1}^3 m_i\mathbf{r}_i\bigr)/m$ is the radius vector of the center of mass of the moving platform with omniwheels, $\mathbf{I}=\mathbf{I}_{\mathrm{p}}+\sum_{i=1}^3\mathbf{I}_i$ is the tensor of inertia of the moving platform with omniwheels with

respect to the center of the sphere, m_i and $\mathbf{I}_i$ are the mass of the ith wheel and its tensor of inertia with respect to the point C, and j is the axial moment of inertia of the wheels.

Using this notation, we can represent the potential energy of the system as

$$U = mg(\mathbf{r}_{\mathrm{m}}, \boldsymbol{\gamma}), \tag{3.3}$$

where g is the acceleration of gravity.

Defining the Lagrange function $L = T - U$ by relations (3.2) and (3.3), substituting it into equations (3.1), and taking into account the indeterminate multipliers found from the last two equations in (3.1) and the time derivative of the constraint equations (2.4), we obtain

$$\begin{aligned}
&(\mathbf{I} + \mathbf{J}_{\mathrm{ss}} - \mathbf{J}_{\mathrm{ns}} - \mathbf{J}_{\mathrm{sn}})\dot{\boldsymbol{\omega}} + \big(\mathbf{J}_{\mathrm{ns}} - \mathbf{J}_{\mathrm{ss}} + mR_0((\boldsymbol{\gamma}, \mathbf{r}_{\mathrm{m}}) - \boldsymbol{\gamma} \otimes \mathbf{r}_{\mathrm{m}})\big)\dot{\boldsymbol{\Omega}} \\
&\quad = -\sum_{i=1}^{3} k_i \mathbf{s}_i K_i - \boldsymbol{\omega} \times \mathbf{I}\boldsymbol{\omega} + (\mathbf{J}_{\mathrm{ns}}(\boldsymbol{\Omega} - \boldsymbol{\omega})) \times \boldsymbol{\omega} - mR_0 \mathbf{r}_{\mathrm{m}} \times (\boldsymbol{\gamma} \times (\boldsymbol{\Omega} \times \boldsymbol{\omega})) - mg(\mathbf{r}_{\mathrm{m}} \times \boldsymbol{\gamma}), \\
&\big(\mathbf{J}_{\mathrm{sn}} - \mathbf{J}_{\mathrm{ss}} + mR_0((\mathbf{r}_{\mathrm{m}}, \boldsymbol{\gamma}) - \mathbf{r}_{\mathrm{m}} \otimes \boldsymbol{\gamma})\big)\dot{\boldsymbol{\omega}} + \big(I_0 + \mathbf{J}_{\mathrm{ss}} + (m + m_0){R_0}^2(\boldsymbol{\gamma}^2 - \boldsymbol{\gamma} \otimes \boldsymbol{\gamma})\big)\dot{\boldsymbol{\Omega}} \\
&\quad = -(m + m_0){R_0}^2 \boldsymbol{\gamma} \times (\boldsymbol{\gamma} \times (\boldsymbol{\Omega} \times \boldsymbol{\omega})) - mR_0(\boldsymbol{\gamma} \times (\boldsymbol{\omega} \times (\boldsymbol{\omega} \times \mathbf{r}_{\mathrm{m}}))) - I_0 \boldsymbol{\omega} \times \boldsymbol{\Omega} + \sum_{i=1}^{3} k_i \mathbf{s}_i K_i
\end{aligned} \tag{3.4}$$

with $k_i = R_0/(R_{\mathrm{w}}(\mathbf{s}_i, \mathbf{n}_i))$, $\mathbf{J}_{\mathrm{ss}} = \sum_{i=1}^{3} jk_i^2(\mathbf{s}_i \otimes \mathbf{s}_i)$, $\mathbf{J}_{\mathrm{sn}} = \sum_{i=1}^{3} jk_i(\mathbf{s}_i \otimes \mathbf{n}_i)$, $\mathbf{J}_{\mathrm{ns}} = \sum_{i=1}^{3} jk_i(\mathbf{n}_i \otimes \mathbf{s}_i)$ and with the tensor product of vectors $\mathbf{a}$ and $\mathbf{b}$ defined as $\mathbf{a} \otimes \mathbf{b} = \|a_i b_j\|$. Combined with the Poisson equation (one of equations in (2.2))

$$\dot{\boldsymbol{\gamma}} = \boldsymbol{\gamma} \times \boldsymbol{\omega}, \tag{3.5}$$

equations (3.4) form a closed reduced system of equations.

In [14], to calculate the controls for the motion of a spherical robot along a given trajectory, we developed an algorithm based on the numerical solution of the system supplemented with initial conditions. Numerical simulation has shown that at the final instant of time, after switching off the control, the internal omniwheel platform is not at rest, which generally leads to chaotic motion of the spherical robot. To eliminate this drawback, we propose a control algorithm that involves basic manoeuvres, called gaits.

4. CONTROL BY MEANS OF GAITS

This method consists in calculating controls under which the spherical robot at the initial and final instants of time certainly moves along some stationary solution (for example, remains at rest). In this case, the trajectory of the spherical robot during a manoeuvre is not specified in advance, and the control problem reduces to choosing a manoeuvre such that the final trajectory of the spherical robot satisfies necessary requirements. Consider an algorithm for searching an appropriate manoeuvre that connects two motions along a straight line.

Motions along a straight line correspond to fixed points of the system (3.4), (3.5) and are parameterized by four quantities: the velocity v of motion along a straight line, the angle δ between the straight line and the axis OX, the angular velocity Ω_γ of "slipping" of the shell at the point of contact with the plane, and the constant precession angle ψ, which defines the orientation of the omniwheel platform during motion. Note that the two other Euler angles θ and φ are also constant during the motion along a straight line and are defined by the vector $\boldsymbol{\gamma} \parallel \mathbf{r}_{\mathrm{m}}$. These parameters are related to the vectors $\boldsymbol{\alpha}$, $\boldsymbol{\beta}$, $\boldsymbol{\gamma}$, and $\boldsymbol{\Omega}$ as follows:

$$\boldsymbol{\Omega} = \Omega_\gamma \boldsymbol{\gamma} + \frac{v}{R_0}(\cos(\delta)\boldsymbol{\beta} - \sin(\delta)\boldsymbol{\alpha}), \qquad \tan\psi = -\frac{\beta_3}{\alpha_3}. \tag{4.1}$$

It is easy to show that the following proposition is valid.

Proposition. *Suppose that for $t < 0$ the spherical robot moves along a straight line with parameters v_0, δ_0, $\Omega_{\gamma 0}$, and ψ_0. In addition, let the robot execute a manoeuvre with given vector $\boldsymbol{\gamma}$ and quantity ω_γ defined as functions of time*

$$\boldsymbol{\gamma} = \boldsymbol{\gamma}(t), \qquad \omega_\gamma = \omega_\gamma(t), \qquad t \in [0, T],$$

such that

$$\boldsymbol{\gamma}(0) = \boldsymbol{\gamma}(T) = \frac{\mathbf{r}_{\mathrm{m}}}{|\mathbf{r}_{\mathrm{m}}|}, \qquad \dot{\boldsymbol{\gamma}}(0) = \dot{\boldsymbol{\gamma}}(T) = 0, \qquad \omega_\gamma(0) = \omega_\gamma(T) = 0.$$

Then, after executing the manoeuvre (for $t > T$), the spherical robot will move along a straight line with the parameters v_{f}, δ_{f}, $\Omega_{\gamma \mathrm{f}}$, and ψ_{f} related to the vectors $\boldsymbol{\alpha}(T)$, $\boldsymbol{\beta}(T)$, and $\boldsymbol{\Omega}(T)$ by formulas similar to (4.1). *In this case, the functions of time $\boldsymbol{\alpha}(t)$, $\boldsymbol{\beta}(t)$, and $\boldsymbol{\Omega}(t)$ are found from the solution of the first three equations in system* (3.4) *in which the vector $\boldsymbol{\omega}$ is a known function of time and is expressed in terms of $\boldsymbol{\gamma}(t)$ and $\omega_\gamma(t)$ as follows*:

$$\boldsymbol{\omega}(t) = \boldsymbol{\gamma}(t)\omega_\gamma(t) + \dot{\boldsymbol{\gamma}}(t) \times \boldsymbol{\gamma}(t).$$

The controls that realize this manoeuvre can be obtained by substituting $\boldsymbol{\omega}(t)$, $\boldsymbol{\Omega}(t)$, and $\boldsymbol{\gamma}(t)$ into one of equations (3.4), *and the explicit form of the spherical robot's trajectory that connects the two motions along straight lines can be obtained by integrating the first kinematic equation in* (2.2).

It is convenient to represent the vector $\boldsymbol{\gamma}$ that defines the manoeuvres (gaits) as

$$\boldsymbol{\gamma}(t) = \big(\sin\theta(t)\cos\varphi(t), \sin\theta(t)\sin\varphi(t), \cos\theta(t)\big), \tag{4.2}$$

where the Euler angles $\varphi(t)$ and $\theta(t)$ define the orientation of the moving platform during a manoeuvre.

5. EXPERIMENTAL INVESTIGATIONS

At the Laboratory of Nonlinear Analysis and the Design of New Types of Vehicles, Udmurt State University, an experimental model of a spherical robot with an internal omniwheel platform was constructed. The design of this spherical robot corresponds to the following values of the parameters: the radius, mass, and moment of inertia of the spherical shell are $R_0 = 0.15$ m, $m_0 = 0.8$ kg, and $I_0 = 0.012\ \mathrm{kg} \cdot \mathrm{m}^2$; the radius of omniwheels is $R_{\mathrm{w}} = 0.07$ m; and the radius vectors defining the position of omniwheels and the directions of their axes and the axes of rollers are

$$\mathbf{r}_i = 0.057(\cos\varphi_i, \sin\varphi_i, -1), \quad \mathbf{n}_i = \frac{1}{\sqrt{2}}(\cos\varphi_i, \sin\varphi_i, 1), \quad \boldsymbol{\alpha}_i = \frac{1}{\sqrt{2}}\Big(\cos\Big(\varphi_i - \frac{\pi}{4}\Big), \sin\Big(\varphi_i - \frac{\pi}{4}\Big), 1\Big),$$

where $\varphi_i = 2\pi(i-1)/3$, $i = 1, 2, 3$; the mass and the tensor of the moving platform with omniwheels are $m = 2.5$ kg and $\mathbf{I} = \mathrm{diag}(0.016, 0.016, 0.023)\ \mathrm{kg} \cdot \mathrm{m}^2$. All experimental investigations were carried out with this model.

To determine the deviations of the real trajectory of the spherical robot from a given trajectory for which the calculations of the controls were made, a motion capture system was used to determine the coordinates of the center of the spherical robot and the orientation of the internal moving platform. To this end, the spherical shell was fabricated of a transparent material (polyethylene terephthalate), and the internal omniwheel platform was supplied with light-retroreflective markers. The cameras of the capture system fixed the position of each marker with frequency of 100 Hz; these data were processed by special software, and the trajectory of the geometric center of the object bounded by the markers was constructed.

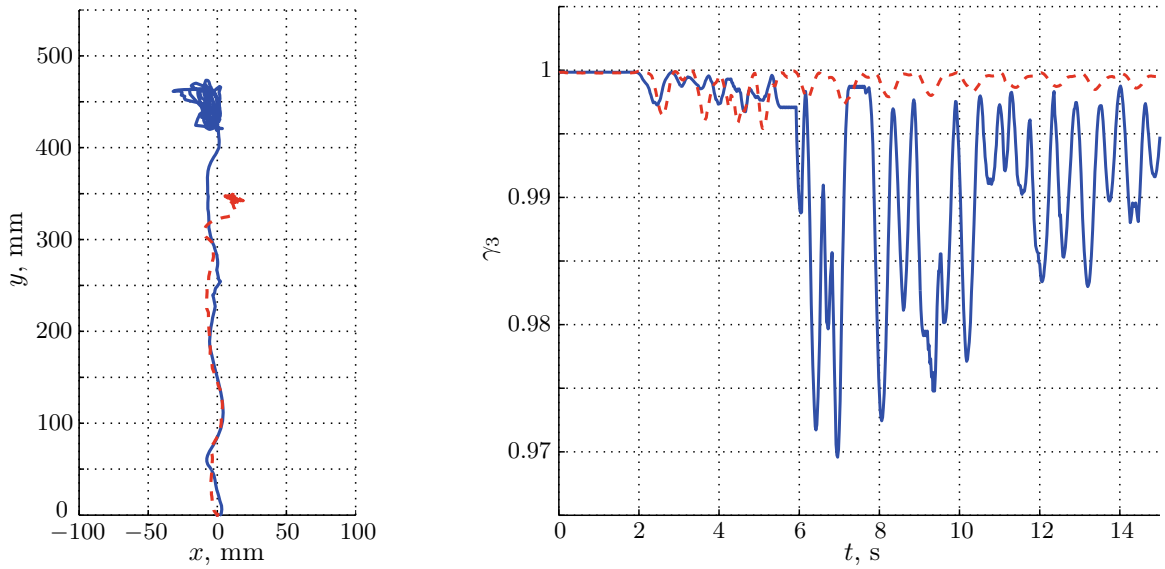

Fig. 2. Comparison of experimental data on the motion of a spherical robot under controls calculated within the kinematic (solid line) and dynamic (dashed line) models for the motion along a straight line segment: (a) trajectories of motion and (b) components of the vector γ_3.

5.1. Comparison of controls within the kinematic and dynamic models. The experimental investigations of the motion of a spherical robot along a straight line and a circle under controls calculated according to the kinematic model are reported in [14]; however, experiments on the investigation of motion within the dynamic model were not carried out there. Figure 2 presents the comparison results for the motion of the spherical robot under controls calculated within the kinematic model and under control by means of gaits.

In the case of the dynamic model, the motion consisted of two manoeuvres that resulted in acceleration from rest to velocity Ω_l and stopping. Each manoeuvre can be defined by the functions $\varphi(t)$, $\theta(t)$, and $\omega_\gamma(t)$.

During acceleration from rest, these functions have the form

$$\theta(t) = \theta_{\max}\sin^2(\pi t), \qquad \varphi(t) = \varphi_0 = 0, \qquad \omega_\gamma(t) = 0, \qquad t \in [0,2], \tag{5.1}$$

where $\theta_{\max}$ is set equal to 0.1 in numerical calculations and the angle φ_0 defines the direction of motion. Acceleration from rest corresponds to the following initial conditions:

$$\Omega_0 = 0, \qquad \boldsymbol{\alpha}_0 = (1,0,0), \qquad \boldsymbol{\beta}_0 = (0,1,0). \tag{5.2}$$

For braking to rest, the functions have the form

$$\theta(t) = -\theta_{\max}\sin^2(\pi t), \qquad \varphi(t) = \varphi_0 = 0, \qquad \omega_\gamma(t) = 0, \qquad t \in [0,2]. \tag{5.3}$$

The initial conditions for braking are

$$\boldsymbol{\Omega}_0 = (0,\Omega_l,0), \qquad \boldsymbol{\alpha}_0 = (1,0,0), \qquad \boldsymbol{\beta}_0 = (0,1,0), \tag{5.4}$$

where Ω_l is the angular velocity of the spherical shell at the start of braking. If we assume that the spherical robot starts braking immediately after the acceleration (5.1), (5.2), then, solving system (3.4), (3.5) numerically, we obtain $\Omega_l = 0.864\ \mathrm{s}^{-1}$.

Within the kinematic model, the motion was defined by the constant angular velocity $\Omega = \Omega_l = 0.864\ \mathrm{s}^{-1}$ during 4 s, which corresponded to the execution time of two manoeuvres within the

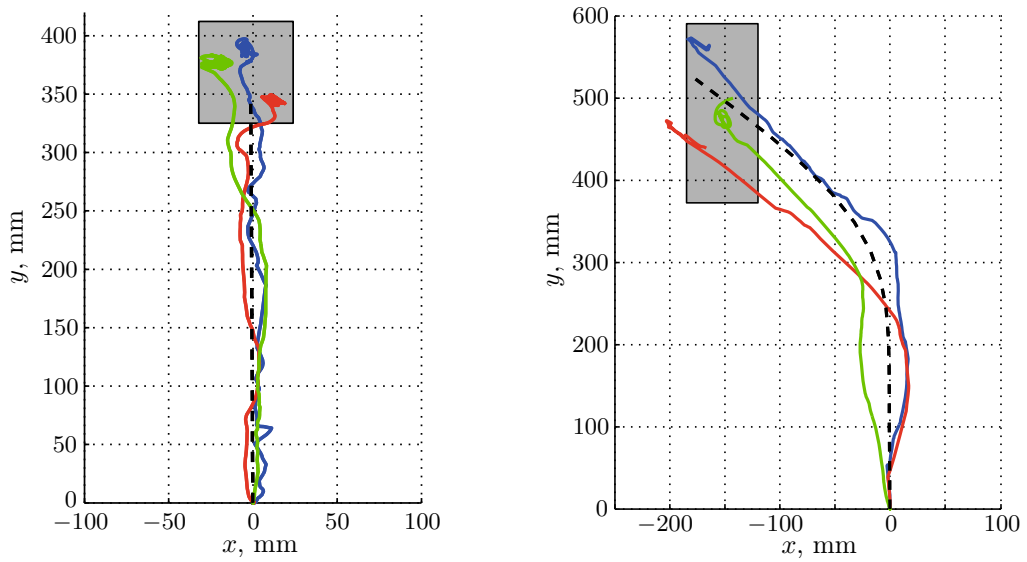

Fig. 3. Trajectories of the motion of a spherical robot under controls calculated within the dynamic model with the use of gaits: (a) rectilinear motion and (b) rectilinear motion combined with a turn. The dashed line represents the result of numerical simulation, and the solid lines demonstrate typical trajectories of the spherical robot.

dynamic model. This motion was defined by a trajectory in the form of a straight line segment along the OY axis:

$$x = 0, \qquad y = 0.13\,t, \qquad \omega_\gamma = 0, \qquad \Omega_\gamma = 0, \qquad t \in [0, 4], \tag{5.5}$$

and the controls were calculated by the expression (2.9).

The experimental trajectories of motion and the γ_3-component of the vector restored by the motion capture system are presented in Fig. 2. The solid line demonstrates the trajectory and the γ_3-component of the vector for the motion within the kinematic model. The motion of the robot lasted 4 s, after which the omniwheels stopped, while the spherical shell continued an oscillatory motion. The figure shows that within the dynamic model of motion, the oscillations after stopping occurred with smaller amplitude and were damped faster. To evaluate the amplitude of these oscillations, we calculate the root mean square deviation for the γ_3-component of the vector after the stopping time of the spherical robot. For the control within the kinematic model, this deviation was $\sigma^{\mathrm{kin}}_{\gamma_3,\,t>4} = 0.018$; within the dynamic model, it was $\sigma^{\mathrm{dyn}}_{\gamma_3,\,t>4} = 0.001$. The results obtained demonstrate the advantages of the dynamic model, and the development of the basic dynamic manoeuvres—acceleration, braking, and turn—allows one to significantly increase the accuracy with which the spherical robot passes along a trajectory, thus complementing or completely replacing the kinematic control model.

5.2. Experimental investigations of the motion under control with the use of gaits. Next, consider the trajectories of motion under control by gaits in more detail and analyze the deviations of the experimental data from the theoretical (prescribed) ones.

1. *Motion along a straight line.* The motion along a straight line was defined by two manoeuvres, acceleration and stopping, which are described by the expressions (5.1), (5.2) and (5.3), (5.4). Figure 3 demonstrates the results of a series of experiments carried out under identical conditions; the dashed line shows a trajectory obtained by numerical simulation, and the solid lines represent typical trajectories of the spherical robot.

The results of the experimental investigations are presented in Fig. 3a. For the stopping point, we constructed confidence intervals calculated for a probability of 95% by the standard deviation for five experiments. For the motion along a straight line, the stop coordinates of the spherical robot under simulation are $x_\mathrm{t} = -0.0695$ mm and $y_\mathrm{t} = 344.6$ mm, while in the experiment we obtained $x_\mathrm{e} = -1.392 \pm 28.9$ mm and $y_\mathrm{e} = 369.2 \pm 37.7$ mm.

2. *Rectilinear motion combined with a turn.* The next experiment included three manoeuvres: acceleration from rest of the form (5.1), (5.2), a turn defined by the expressions

$$\theta(t) = \theta_{\max} \sin^2(\pi t), \qquad \varphi(t) = \varphi_{90} = \frac{\pi}{2}, \qquad \omega_\gamma(t) = 0, \qquad t \in [0, 2], \tag{5.6}$$

with the initial conditions (5.4), and braking of the form (5.3) but for $\varphi(t) = \pi/4$ and with the initial conditions

$$\boldsymbol{\Omega}_0 = (0.868, 0.852, 0), \qquad \boldsymbol{\alpha}_0 = (1, 0, 0), \qquad \boldsymbol{\beta}_0 = (0, 1, 0). \tag{5.7}$$

The results of the experimental investigations are presented in Fig. 3b. For the rectilinear motion followed by a turn according to the manoeuvres (5.1), (5.2), (5.6), and (5.4) and braking with the initial conditions (5.7), numerical simulation yields $x_\mathrm{t} = -173.2$ mm and $y_\mathrm{t} = 519.4$ mm, while in the experiment we obtained $x_\mathrm{e} = -151.3 \pm 32.4$ mm and $y_\mathrm{e} = 482.4 \pm 112.1$ mm. One can see that the coordinates of the stopping points of the spherical robot moving under the control with the use of the gaits obtained by numerical simulation (solution of system (3.4), (3.5)) fall into the given confidence interval.

CONCLUSIONS

In conclusion, we summarize the main results presented in the paper and formulate open questions.

1. We have solved a nonholonomic problem of controlling the motion of a spherical robot with an internal omniwheel platform in the kinematic (quasistatic) and dynamic statements.

2. We have carried out an experimental evaluation test of the theoretical results obtained within the control models developed. We have shown that for technically feasible speeds of motion, these models well agree with the results of experiments.

3. We have shown that a control algorithm using gaits based on the nonholonomic dynamic model allows one to significantly increase the accuracy of following the trajectory and can be used to control a real spherical robot with an internal omniwheel platform.

4. One of the most important conditions for the implementability of the control models developed is the fulfillment of nonholonomic no-slip conditions of the spherical shell on the surface and of the rollers of the omniwheels on the surface of the spherical shell. In laboratory conditions, this was achieved by the choice of the materials of the spherical shell and the rollers. In reality, it is difficult to guarantee these conditions, and possible slipping can be compensated for by introducing feedbacks into the system.

ACKNOWLEDGMENTS

We are grateful to A.V. Borisov and I.S. Mamaev for fruitful discussions of the results.

The work of A.A. Kilin (Sections 2 and 3) is supported by the Russian Foundation for Basic Research, project nos. 15-38-20879-mol_a_ved and 15-08-09261-a. The work of Yu.L. Karavaev (Sections 4 and 5) is supported by the Russian Science Foundation under grant 14-19-01303.

REFERENCES

1. S.-S. Ahn and Y.-J. Lee, "Novel spherical robot with hybrid pendulum driving mechanism," Adv. Mech. Eng. **2014**, 456727 (2014).
2. I. A. Bizyaev, A. V. Borisov, and I. S. Mamaev, "The dynamics of nonholonomic systems consisting of a spherical shell with a moving rigid body inside," Regul. Chaotic Dyn. **19** (2), 198–213 (2014) [Nelinein. Din. **9** (3), 547–566 (2013)].
3. A. V. Borisov, Yu. L. Karavaev, I. S. Mamaev, N. N. Erdakova, T. B. Ivanova, and V. V. Tarasov, "Experimental investigation of the motion of a body with an axisymmetric base sliding on a rough plane," Regul. Chaotic Dyn. **20** (5), 518–541 (2015) [Nelinein. Din. **11** (3), 547–577 (2015)].
4. A. V. Borisov, A. A. Kilin, and I. S. Mamaev, "How to control the Chaplygin ball using rotors. II," Regul. Chaotic Dyn. **18** (1–2), 144–158 (2013) [Nelinein. Din. **9** (1), 59–76 (2013)].
5. A. V. Borisov, A. A. Kilin, and I. S. Mamaev, "Dynamics and control of an omniwheel vehicle," Regul. Chaotic Dyn. **20** (2), 153–172 (2015).
6. A. V. Borisov and I. S. Mamaev, "Equations of motion of non-holonomic systems," Usp. Mat. Nauk **70** (6), 203–204 (2015) [Russ. Math. Surv. **70**, 1167–1169 (2015)].
7. A. V. Borisov and I. S. Mamaev, "Notes on new friction models and nonholonomic mechanics," Usp. Fiz. Nauk **185** (12), 1339–1341 (2015) [Phys. Usp. **58**, 1220–1222 (2015)].
8. A. V. Borisov, I. S. Mamaev, and I. A. Bizyaev, "The Jacobi integral in nonholonomic mechanics," Regul. Chaotic Dyn. **20** (3), 383–400 (2015) [Nelinein. Din. **11** (2), 377–396 (2015)].
9. R. Chase and A. Pandya, "A review of active mechanical driving principles of spherical robots," Robotics **1** (1), 3–23 (2012).
10. W.-H. Chen, C.-P. Chen, W.-S. Yu, C.-H. Lin, and P.-C. Lin, "Design and implementation of an omnidirectional spherical robot Omnicron," in *Proc. 2012 IEEE/ASME Int. Conf. on Advanced Intelligent Mechatronics, Kaohsiung (Taiwan), 2012* (IEEE, Piscataway, NJ, 2012), pp. 719–724.
11. V. A. Crossley, "A literature review on the design of spherical rolling robots," Preprint (Carnegie Mellon Univ., Pittsburgh, PA, 2006).
12. F. R. Hogan and J. R. Forbes, "Modeling of spherical robots rolling on generic surfaces," Multibody Syst. Dyn. **35** (1), 91–109 (2015).
13. T. B. Ivanova and E. N. Pivovarova, "Comments on the paper by A.V. Borisov, A.A. Kilin, I.S. Mamaev 'How to control the Chaplygin ball using rotors. II'," Regul. Chaotic Dyn. **19** (1), 140–143 (2014) [Nelinein. Din. **10** (1), 127–132 (2014)].
14. Yu. L. Karavaev and A. A. Kilin, "The dynamics and control of a spherical robot with an internal omniwheel platform," Regul. Chaotic Dyn. **20** (2), 134–152 (2015) [Nelinein. Din. **11** (1), 187–204 (2015)].
15. J. Lee and W. Park, "Design and path planning for a spherical rolling robot," in *Proc. ASME 2013 International Mechanical Engineering Congress and Exposition* (ASME, 2013, paper no. IMECE2013-64994).
16. M. Svinin, Y. Bai, and M. Yamamoto, "Dynamic model and motion planning for a pendulum-actuated spherical rolling robot," in *Robotics and Automation: Proc. 2015 IEEE Int. Conf. (ICRA)* (IEEE, Piscataway, NJ, 2015), pp. 656–661.
17. T. Ylikorpi, P. Forsman, A. Halme, and J. Saarinen, "Unified representation of decoupled dynamic models for pendulum-driven ball-shaped robots," in *Proc. 28th Eur. Conf. on Modelling and Simulation, Brescia, 2014* (ECMS, 2014), pp. 411–420.
18. T. Ylikorpi and J. Suomela, "Ball-shaped robots," in *Climbing and Walking Robots: Towards New Applications*, Ed. by H. Zhang (I-Tech Educ. Publ., Vienna, 2007), pp. 235–256.
19. T. Yu, H. Sun, Q. Jia, Y. Zhang, and W. Zhao, "Stabilization and control of a spherical robot on an inclined plane," Res. J. Appl. Sci. Eng. Technol. **5** (6), 2289–2296 (2013).
20. Q. Zhan, "Motion planning of a spherical mobile robot," in *Motion and Operation Planning of Robotic Systems: Background and Practical Approaches* (Springer, Cham, 2015), pp. 361–381.
21. M. Zheng, Q. Zhan, J. Liu, and Y. Cai, "Control of a spherical robot: Path following based on nonholonomic kinematics and dynamics," Chin. J. Aeronaut. **24** (3), 337–345 (2011).

Translated by I. Nikitin